JACS
JOURNAL OF THE AMERICAN CHEMICAL SOCIETY

Communication

pubs.acs.org/JACS

Determination of Specific Binding Interactions at L-Cystine Crystal Surfaces with Chemical Force Microscopy

Trinanjana Mandal and Michael D. Ward*

Department of Chemistry and the Molecular Design Institute, New York University, 100 Washington Square East, New York, New York 10003-6688, United States

Supporting Information

ABSTRACT: The pathogenesis of L-cystine kidney stones involves four critical steps: nucleation, crystal growth, crystal aggregation, and crystal adhesion to cells. Although inhibition of crystal growth by L-cystine "imposters" at L-cystine crystal surfaces has been suggested as a plausible route for the suppression of stones, understanding the factors that govern crystal−crystal aggregation and adhesion of crystals to epithelial cells also is essential for devising strategies to mitigate L-cystine stone formation. Chemical force microscopy performed with atomic force microscope tips decorated with functional groups commonly found in urinary constituents that likely mediate aggregation and attachment (e.g., COOH, NH_2, SH, CH_3, OH) revealed signatures that reflect differences in the chemical affinity of these groups for the (001) and {100} faces of the naturally occurring hexagonal form of L-cystine single crystals and the {110} faces of the non-native tetragonal form. These signatures can be explained by the different chemical compositions of the crystal faces, and they reveal a remarkable binding specificity of the thiol group for the sulfur-rich {100} and {110} faces of the hexagonal and tetragonal forms, respectively. Collectively, these observations suggest that alterations of the crystal habit and polymorph by crystal growth inhibitors may not affect crystal aggregation or adhesion to cells significantly.

Cystinuria is a hereditary disorder that affects approximately 20,000 individuals in the United States alone.[1] This debilitating disease, which results from a mutation in either the SLC3A1 gene on chromosome 2 or the SLC7A9 gene on chromosome 19, is a consequence of impaired reabsorption of cystine, ornithine, arginine, and lysine amino acids in the nephron and gastrointestinal tract.[2] The negligible solubility of L-cystine under the conditions existing in the kidney and bladder is conducive to crystallization and formation of stones,[3] which are aggregates of single crystals. Scanning electron microscopy has revealed that L-cystine stones comprise stacks of {001} platelets of the hexagonal form of L-cystine ($P6_122$ space group; $a = b = 0.5422$ nm, $c = 5.6275$ nm); crystals grown from aqueous solutions exhibit a similar habit, with large hexagonal {001} faces bounded by narrow {100} faces (Figure 1A). Treatments for L-cystine stone prevention include dilution through high fluid intake,[4] increasing urine pH through ingestion of alkalinizing potassium or sodium salts,[5] or the administration of thiol drugs such as D-penicillamine and α-mercaptopropionylglycine, which react with L-cystine to generate more soluble asymmetric disulfides. These treatments suppress but typically do not completely prevent stone formation and are limited by lack of patient adherence, adverse side effects, and a failure to stop the recurrence of stones.[4]

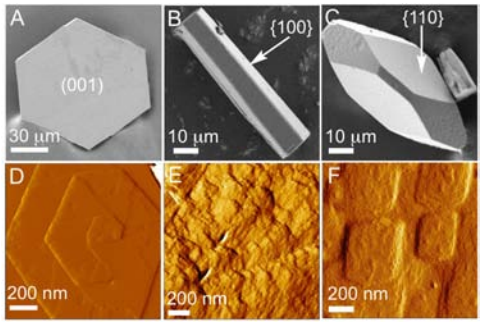

Figure 1. (Top) Scanning electron microscopy images of hexagonal L-cystine crystals: (A) hexagonal plate with a dominant (001) face, grown from an aqueous solution of L-cystine; (B) hexagonal needle grown in the presence of 1% L-CDME, with six dominant {100} faces; (C) tetragonal L-cystine grown in the presence of 3% L-CDME, with four dominant {110} faces. (Bottom) AFM images of the (D) hexagonal (001), (E) hexagonal {100}, and (F) tetragonal {110} faces of L-cystine collected in 2 mM L-cystine solution (pH ≈ 7).

Our laboratory recently reported that low concentrations of the methyl and dimethyl esters of L-cystine (L-CME and L-CDME, respectively) significantly inhibited L-cystine crystal growth by acting as "molecular imposters" that bind to crystal step sites and block the attachment of incoming L-cystine solute molecules, resulting in substantial reductions in the overall crystal yields and suggesting a possible therapy for L-cystine stone prevention.[6] Moreover, these inhibitors dramatically affected the crystal habit, producing small hexagonal rods (Figure 1B) rather than the customary large hexagonal plates. The volume of each hexagonal rod was typically 1/1000 of the volume of the platelike crystals grown in the absence of the inhibitor. Notably, at high concentrations L-CDME produces the tetragonal polymorph of L-cystine as well as the hexagonal form. The tetragonal form has large {110} faces (Figure 1C). It is reasonable to suggest that the crystallographically unique crystal faces of the hexagonal and tetragonal forms have different adhesion characteristics because of their distinct

Received: February 5, 2013
Published: April 4, 2013

 © 2013 American Chemical Society dx.doi.org/10.1021/ja401309d | J. Am. Chem. Soc. 2013, 135, 5525−5528

chemical compositions, which may be critical to cell adhesion and aggregation in vivo.

Urinary macromolecules are thought to play an important role in crystal−crystal aggregation, acting as "glue" that binds crystal surfaces. Chemical force microscopy (CFM)[7,8] performed on these different crystal faces with atomic force microscope (AFM) tips modified with functional groups existing in urinary constituents can produce insight into stone formation events that rely on adhesion. For example, the stronger adhesion forces observed on calcium oxalate monohydrate (COM) compared with calcium oxalate dihydrate surfaces provided an explanation for the greater propensity of COM to form stones.[9] Others have used CFM methods to study the adhesive properties of cholesterol monohydrate, uric acid, and monosodium urate monohydrate crystal surfaces.[10]

AFM tips with terminal carboxylic acid, amine, methyl, or hydroxyl groups were prepared by immersing gold-coated Si_3N_4 tips in 1 mM ethanolic solutions of various ω-functionalized thiols for 18 h.[11] Tips with sulfhydryl groups were obtained using a previously reported protocol [Scheme S1 in the Supporting Information (SI)].[12] L-Cystine crystals were affixed to an AFM sample stage with a partially UV-cured adhesive, which was then cured completely to bond the crystals to the sample stage. The functionalized tips were brought into contact with hexagonal (001), hexagonal {100}, and tetragonal {110} faces of L-cystine crystals submerged in a saturated aqueous solution of L-cystine (0.5 mM, pH ≈ 7). The crystal surfaces were stable under these conditions with no observable motion of steps or changes in step density and orientation. Care was taken to locate the AFM tip over a flat terrace prior to collection of each set of AFM force data in order to minimize the influence of step edges on the adhesion forces. The tip was allowed to contact the crystal surface for a dwell time of 4 s and then retracted to detach it from the surface. A total of 800−1000 pull-off forces were measured for each tip−sample combination at 16−20 different locations on the crystal face (Table S1 in the SI). The forces were collected into a histogram, and the mean value of the force, the standard deviation, and the standard error were calculated. More than 95% of the individual force values for a specific tip−crystal combination fell within the normal distribution curve, reflecting small variances.

The adhesion forces measured with tips decorated with terminal COO^- and NH_3^+ groups were larger on all three crystal faces than for tips decorated with terminal OH and CH_3 groups (Figure 2). Aliphatic carboxylic acids and amines typically have surface pK_a values close to 5−6 and 6−8, respectively.[13,14] Therefore, it is reasonable to expect that at pH ≈ 7 the carboxylic acid and amine tips are charged to some extent. The terminal SH group exhibits stronger adhesion forces toward the hexagonal {100} and tetragonal {110} faces than toward the hexagonal {001} faces. Tips terminated with OH and CH_3 groups exhibit weak forces of adhesion toward all of the examined crystal faces, reflecting the absence of specific interactions between the tip and the crystal surfaces (Table S1).

Stronger adhesion forces typically correspond to specific interactions between the CFM tip and the crystal surface. The structure of the hexagonal form of L-cystine reveals that L-cystine molecules are organized as a helix about the 6_1 screw axis with six cystine molecules spanning the ∼5.6 nm unit cell length along the *c* axis.[15] The L-cystine molecules exhibit intermolecular $NH_3^+\cdots COO^-$ hydrogen bonding along the 6_1 screw axis, intermolecular S···S interactions normal to the {100} planes, and $NH_3^+\cdots COO^-$ hydrogen bonding between adjacent helices in the *ab* (001) plane.

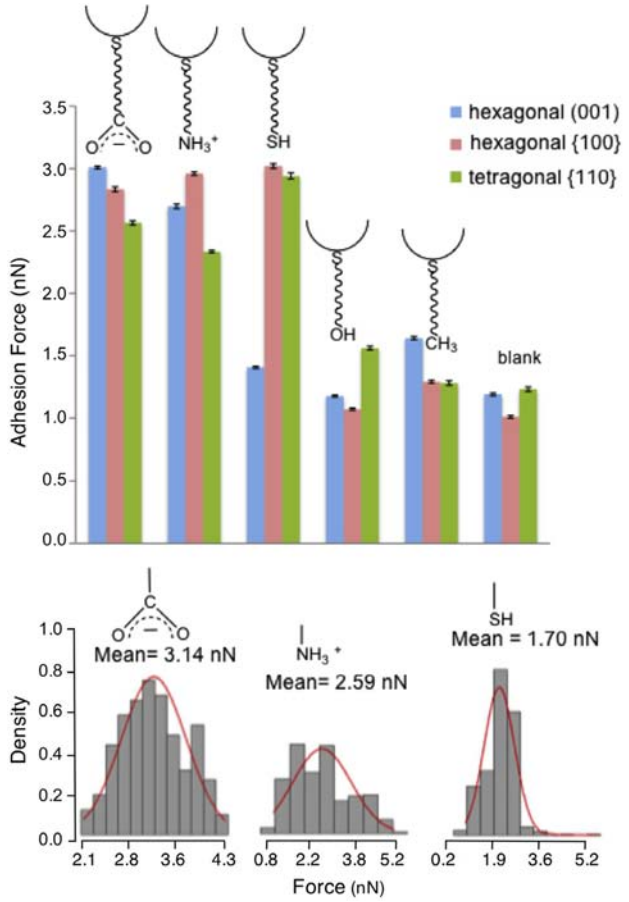

Figure 2. (Top) Mean adhesion forces for the (001) and {100} faces of hexagonal L-cystine crystals and the {110} faces of tetragonal L-cystine crystals using AFM tips decorated with various functional groups. The measurements were performed in an aqueous solution containing 0.5 mM L-cystine using a trigger point of 2 nN and a dwell time of 4 s. Error bars represent the standard error of the mean (standard deviation divided by square root of sample size) calculated from the force histograms. (Bottom) Characteristic histograms for the hexagonal L-cystine (001) surface and tips decorated with COO^-, SH, and NH_3^+. The red traces represent the normal distribution function; all of the measurements were included in these histograms. The values in the top panel represent averages of two or three sets of measurements performed with independent tip−crystal combinations, whereas the mean values above the histograms in the bottom panel correspond to a single tip−crystal combination.

The topography of the hexagonal (001) face (Figure 1D) exhibits flat terraces separated by steps with heights of 5−6 nm, corresponding to the unit cell length *c*. The (001) terraces expose COO^- and NH_3^+ groups, whereas the sulfur atoms are present on {100} steps only. A CFM tip approaching a hexagonal {001} face is more likely to interact with the COO^- and NH_3^+ moieties on the terrace than the disulfide groups exposed at the steps (Figure 3A). This explains the weaker adhesion force between the SH-terminated tip and the {001} faces. Conversely, the hexagonal {100} faces expose COO^-, NH_3^+, *and* disulfide groups, making all three groups available for adhesion (Figure 3B). This explains the stronger adhesion force between the SH-terminated tips and the hexagonal {100} face compared with the {001} surface, supporting specific and

dx.doi.org/10.1021/ja401309d | J. Am. Chem. Soc. 2013, 135, 5525−5528

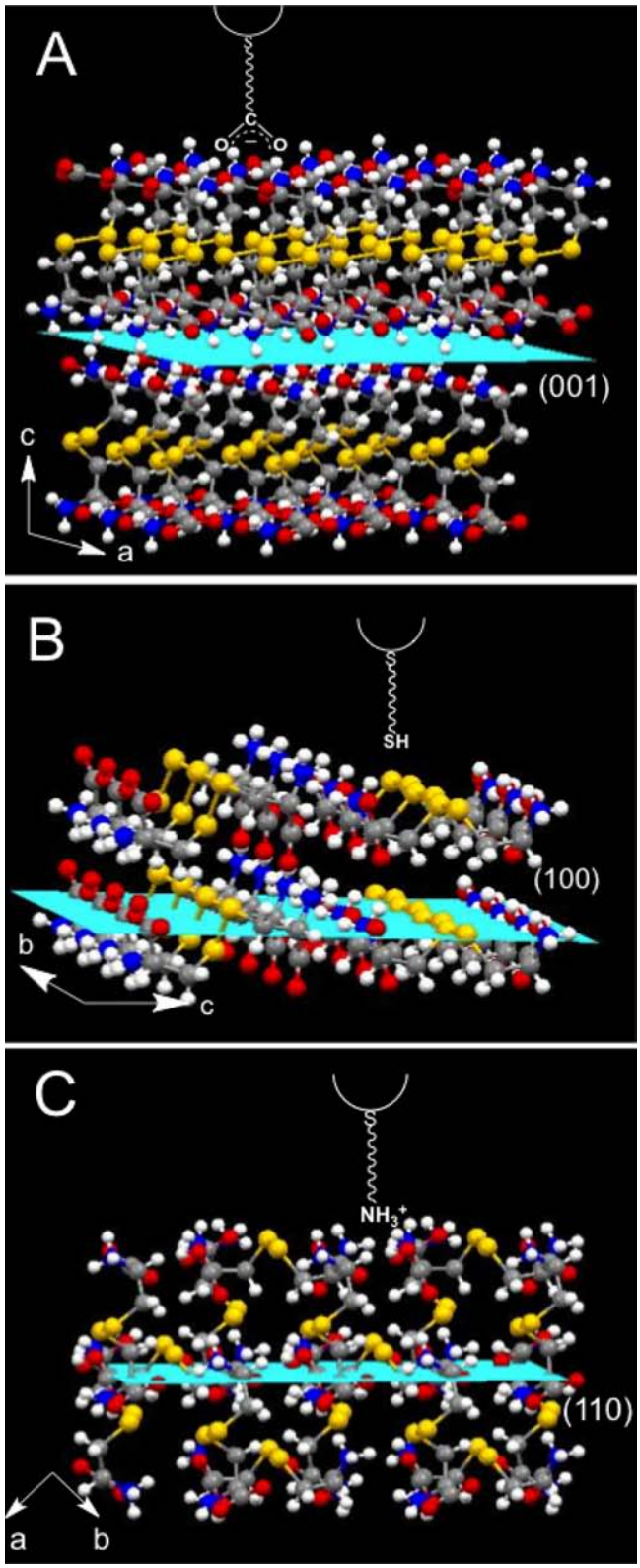

Figure 3. Representations of functionalized CFM tips approaching (A) the (001) face of the hexagonal form of L-cystine, (B) the {100} face of the hexagonal form, and (C) the {110} face of the tetragonal form. Atom color code: carbon (gray), hydrogen (white), nitrogen (blue), oxygen (red), sulfur (yellow). The light-blue planes are visual aids to illustrate the respective crystal planes.

significant interactions between the SH group and the disulfide groups exposed at the {100} crystal surface.

The structure of the tetragonal polymorph of L-cystine[16] ($P4_1$; $a = b = 0.6710$ nm, $c = 2.173$ nm) reveals that four L-cystine molecules wind about the 4_1 screw axis along *c*, with the disulfide bonds contained within each of the four {110} faces (Figure 3C). Intermolecular $NH_3^+\cdots COO^-$ hydrogen bonding is perpendicular to the screw axis in the *ab* plane and also between adjacent amino and carboxylate groups along *c*. The {110} face of tetragonal L-cystine possesses sites with COO^-, NH_3^+, and disulfide groups and displays stronger adhesion toward tips terminated with COO^-, NH_3^+, and SH compared with tips bearing OH and CH_3 pendant groups. We note that the step density of the hexagonal {100} surface (Figure 1E) is somewhat larger than that of hexagonal (001), but step-free flat areas were easily located. The tetragonal {110} surfaces exhibited substantially larger step density (Figure 1F). However, bare tips and tips decorated with nonspecific methyl groups exhibited similar adhesion forces on all three faces, suggesting that the larger step density on tetragonal {110} surfaces does not exert an appreciable influence.

The observations described above demonstrate the capability of CFM to distinguish chemical recognition events occurring on different crystal planes exposed on the faces of a molecular crystal. While the actual values of the force vary somewhat for different tips and L-cystine crystals of the same form, the trends described above are reproducible. The stronger adhesion forces observed with COO^-, NH_3^+, and SH functional groups indicate that an effective molecular inhibitor is one that permits hydrogen bonding and S···S interactions between the inhibitor and chemical groups exposed at the L-cystine crystal surfaces. The CFM data support our earlier suggestion that L-CDME inhibits the growth of the hexagonal form by binding to two specific L-cystine sites (among the six possible) that expose disulfide groups on the flanks of the {100} steps.[6] The results also suggest that the changes in the crystal habit of hexagonal L-cystine caused by the molecular imposters, wherein the {100} faces become more dominant than the {001} faces, would not produce crystals that are more adhesive toward common functional groups in urinary macromolecules. Moreover, the adhesion forces on the dominant faces of the hexagonal and tetragonal forms are comparable. It is therefore reasonable to conclude that CME and CDME, and related molecular imposters, would not elevate the risk of crystal aggregation and subsequent stone formation, which is promising for their development as therapeutic agents.

■ ASSOCIATED CONTENT

Ⓢ Supporting Information

Materials and methods, including fabrication of modified CFM tips, CFM force measurement protocols, and AFM images of crystal surfaces. This material is available free of charge via the Internet at http://pubs.acs.org.

■ AUTHOR INFORMATION

Corresponding Author

mdw3@nyu.edu

Notes

The authors declare no competing financial interest.

■ ACKNOWLEDGMENTS

This work was supported by the Molecular Design Institute of New York University. The authors gratefully acknowledge Dr. Chunhua Hu for technical assistance. The Zeiss Merlin field-

emission scanning electron microscope was acquired through the support of the National Science Foundation under Award DMR-0923251 with additional contributions from the NSF-supported NYU Materials Research Science and Engineering Center under Award DMR-0820341.

REFERENCES

(1) Ahmed, K.; Dasgupta, P.; Khan, M. S. *Postgrad. Med. J.* **2006**, *82*, 799−801.
(2) (a) Dolin, D. J.; Asplin, J. R.; Flagel, L.; Grasso, M.; Goldfarb, D. S. *J. Endourol.* **2005**, *19*, 429−432. (b) Mattoo, A.; Goldfarb, D. S. *Semin. Nephrol.* **2008**, *28*, 181−191.
(3) Moe, O. W. *Lancet* **2006**, *367*, 333−344.
(4) Becker, G. *Nephrology* **2007**, *12* (Suppl. 1), S4−S10.
(5) Nakagawa, Y.; Asplin, J. R.; Goldfarb, D. S.; Parks, J. H.; Coe, F. L. *J. Urol.* **2000**, *164*, 1481−1485.
(6) Rimer, J. D.; An, Z.; Zhu, Z.; Lee, M. H.; Goldfarb, D. S.; Wesson, J. A.; Ward, M. D. *Science* **2010**, *330*, 337−341.
(7) (a) Noy, A.; Vezenov, D. V.; Lieber, C. M. *Annu. Rev. Mater. Sci.* **1997**, *27*, 381−421. (b) Noy, A. *Surf. Interface Anal.* **2006**, *38*, 1429−1441. (c) Poggi, M. A.; Gadsby, E. D.; Bottomley, L. A.; King, W. P.; Oroudjev, E.; Hansma, H. *Anal. Chem.* **2004**, *76*, 3429−3444.
(8) (a) Florin, E. L.; Moy, V. T.; Gaub, H. E. *Science* **1994**, *264*, 415−417. (b) Lee, G. U.; Chrisey, L. A.; Colton, R. J. *Science* **1994**, *266*, 771−773. (c) Dammer, U.; Hegner, M.; Anselmetti, D.; Wagner, P.; Dreier, M.; Huber, W.; Güntherodt, H. J. *Biophys. J.* **1996**, *70*, 2437−2441. (d) McKendry, R.; Theoclitou, M.-E.; Rayment, T.; Abell, C. *Nature* **1998**, *391*, 566−568.
(9) (a) Sheng, X.; Jung, T.; Wesson, J. A.; Ward, M. D. *Proc. Natl. Acad. Sci. U.S.A.* **2005**, *102*, 267−272. (b) Sheng, X.; Ward, M. D.; Wesson, J. A. *J. Am. Chem. Soc.* **2003**, *125*, 2854−2855. (c) Sheng, X.; Ward, M. D.; Wesson, J. A. *J. Am. Soc. Nephrol.* **2005**, *16*, 1904−1908.
(10) (a) Abendan, R. S.; Swift, J. A. *Langmuir* **2002**, *18*, 4847−4853. (b) Presores, J. B.; Swift, J. A. *Langmuir* **2012**, *28*, 7401−7406. (c) Perrin, C. M.; Swift, J. A. *CrystEngComm* **2012**, *14*, 1709−1715.
(11) Noy, A.; Frisbie, C. D.; Rozsnyai, L. F.; Wrighton, M. S.; Lieber, C. M. *J. Am. Chem. Soc.* **1995**, *117*, 7943−7951.
(12) (a) Smith, E. A.; Thomas, W. D.; Kiessling, L. L.; Corn, R. M. *J. Am. Chem. Soc.* **2003**, *125*, 6140−6148. (b) Smith, E. A.; Wanat, M. J.; Cheng, Y. F.; Barreira, S. V. P.; Frutos, A. G.; Corn, R. M. *Langmuir* **2001**, *17*, 2502−2507.
(13) Chechik, V.; Crooks, R. M.; Stirling, C. J. M. *Adv. Mater.* **2000**, *12*, 1161−1171.
(14) van der Vegte, E. W.; Hadziioannou, G. *J. Phys. Chem. B* **1997**, *101*, 9563−9569.
(15) Oughton, B. M.; Harrison, P. M. *Acta Crystallogr.* **1959**, *12*, 396−404.
(16) Chaney, M. O.; Steinrauf, L. K. *Acta Crystallogr.* **1974**, *B30*, 711−716.